

## Measurement of drift mobility in AlGaN/GaN heterostructure field-effect transistor

X. Z. Dang, P. M. Asbeck, and E. T. Yu<sup>a)</sup>

Department of Electrical and Computer Engineering, University of California at San Diego, La Jolla, California 92093-0407

G. J. Sullivan, M. Y. Chen, and B. T. McDermott  
Rockwell Science Center, Thousand Oaks, California 91358

K. S. Boutros and J. M. Redwing  
Epitronics/ATMI, Phoenix, Arizona 85027-2726

(Received 27 January 1999; accepted for publication 25 April 1999)

Low-field mobilities for electrons in the channel of an  $\text{Al}_{0.15}\text{Ga}_{0.85}\text{N}/\text{GaN}$  heterostructure field-effect transistor are derived from direct current transistor characteristics. The dependencies of mobility on gate bias, sheet carrier concentration, and temperature are obtained. For negative gate bias voltages, mobility is found to increase monotonically with increasing sheet carrier concentration, which we interpret as a consequence of increased screening of carrier scattering. For positive gate bias voltages, mobility is found to decrease with increasing gate bias due to the onset of parallel conduction in the AlGaN barrier layer. The mobility varies approximately as  $T^{-\alpha}$  with  $\alpha \approx 1.6\text{--}1.8$  for temperature ranging from 200 to 400 K, indicating that phonon scattering is dominant in the two-dimensional electron gas in this temperature range. © 1999 American Institute of Physics. [S0003-6951(99)01225-5]

III–V nitrides have attracted intense interest recently for applications in high-temperature, high-power electronic devices operating at microwave frequencies. Great progress has been made in recent years to improve the characteristics of nitride heterostructure field-effect transistors (HFETs).<sup>1–4</sup> However, detailed characterization of electron transport is crucial for further design and optimization of these devices. In this letter, we present detailed measurements of low-field mobility in the channel of an  $\text{Al}_{0.15}\text{Ga}_{0.85}\text{N}/\text{GaN}$  HFET. The dependence of mobility on gate voltage, sheet concentration and temperature is derived from direct current (dc) current–voltage transistor characteristics. Possible mechanisms for the observed dependence of mobility on these factors are investigated.

The  $\text{Al}_{0.15}\text{Ga}_{0.85}\text{N}/\text{GaN}$  heterostructure employed in these studies was grown by metalorganic chemical vapor deposition (MOCVD) on a sapphire substrate, and consisted of a 150-Å-thick AlN buffer layer, a 5  $\mu\text{m}$  nominally undoped GaN buffer layer, followed by a 100 Å nominally undoped  $\text{Al}_{0.15}\text{Ga}_{0.85}\text{N}$  spacer layer, and finally a 300 Å Si-doped  $\text{Al}_{0.15}\text{Ga}_{0.85}\text{N}$  layer with  $n \sim 2 \times 10^{18} \text{ cm}^{-3}$ . The piezoelectric effect<sup>5</sup> combined with intentional doping in the  $\text{Al}_{0.15}\text{Ga}_{0.85}\text{N}$  barrier layer contribute to the formation of a two-dimensional electron gas (2DEG) at the  $\text{Al}_{0.15}\text{Ga}_{0.85}\text{N}/\text{GaN}$  interface. Transistor structures were fabricated with Pt/Au as the gate metal, and Ti/Al/Pt/Au for the ohmic source and drain contacts. Ohmic contacts were annealed at 800 °C for 60 s. Measurements were performed on large-area transistors, with gate lengths of 50  $\mu\text{m}$  and gate widths ranging from 50 to 150  $\mu\text{m}$ ; the source series resistance is estimated to be less than 5  $\Omega \text{ mm}$ .

Sheet carrier concentrations and their vertical distribution within the HFET structure were obtained as a function of gate bias voltage by capacitance–voltage ( $C$ – $V$ ) profiling. Figure 1(a) shows the  $C$ – $V$  characteristic measured between the gate and source of a HFET with a 50  $\mu\text{m} \times 100 \mu\text{m}$  gate; the sheet carrier concentration derived from the  $C$ – $V$  curve is shown by the solid line in Fig. 1(b). A threshold voltage of  $-2.1 \text{ V}$  is obtained. The plateau in capacitance at

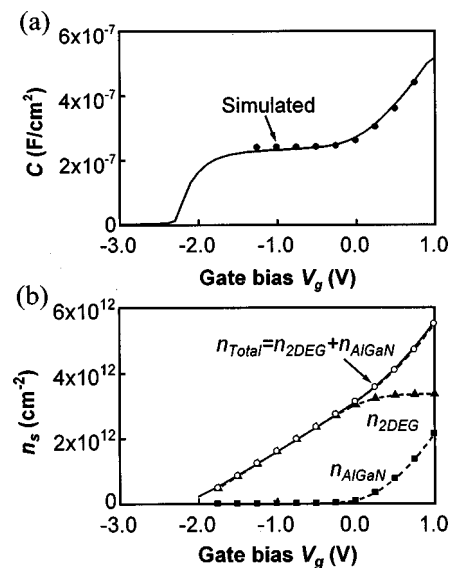


FIG. 1. (a) Measured (solid line) and simulated (circles) capacitance–voltage characteristic between the gate and source of an  $\text{Al}_{0.15}\text{Ga}_{0.85}\text{N}/\text{GaN}$  HFET with a 50  $\mu\text{m} \times 100 \mu\text{m}$  gate. (b) Simulated sheet carrier concentration in the 2DEG (triangles+dashed line) and the AlGaN layer (solid squares+dashed line), and the total sheet concentration (open circles+dashed lines). Simulated values are in good agreement with the measured total sheet carrier concentration (solid line).

<sup>a)</sup>Electronic mail: ety@ece.ucsd.edu

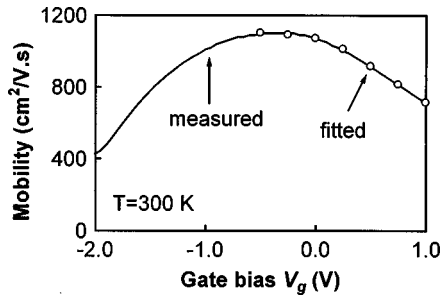


FIG. 2. Electron drift mobility derived from dc transistor characteristics in an  $\text{Al}_{0.15}\text{Ga}_{0.85}\text{N}/\text{GaN}$  HFET with a  $50\ \mu\text{m}\times 100\ \mu\text{m}$  gate as a function of gate bias (line), and fitted mobility values assuming the existence of parallel conduction in the  $\text{AlGaIn}$  layer (circles).

negative gate bias voltages corresponds to the carriers in the 2DEG located at the  $\text{Al}_{0.15}\text{Ga}_{0.85}\text{N}/\text{GaN}$  interface. The concentration of carriers in the 2DEG is  $3.1\times 10^{12}\ \text{cm}^{-2}$  at  $V_g = 0\ \text{V}$ . This is relatively low compared to carrier concentrations that have often been reported for  $\text{AlGaIn}/\text{GaN}$  HFETs;<sup>3</sup> we attribute this difference primarily to low dopant concentrations and the relatively low Al concentration in our sample structure. For positive gate bias voltages, a rapid increase in capacitance with increasing  $V_g$  occurs, indicating that the carrier distribution has shifted toward the Schottky contact. Numerical simulations of capacitance and sheet carrier concentration have been performed using a one-dimensional Poisson/Schrödinger solver.<sup>6</sup> As shown in Figs. 1(a) and 1(b), the simulated capacitance and total sheet carrier concentration, when a thickness of 330 Å and doping level of  $1.8\times 10^{18}\ \text{cm}^{-3}$  are assumed for the  $\text{Al}_{0.15}\text{Ga}_{0.85}\text{N}$  barrier layer, are in excellent agreement with measured values. The simulated carrier distributions between the 2DEG and  $\text{Al}_{0.15}\text{Ga}_{0.85}\text{N}$  layer confirm that substantial spillover of carriers into the  $\text{Al}_{0.15}\text{Ga}_{0.85}\text{N}$  layer occurs for  $V_g \geq 0\ \text{V}$ , resulting in an increase in gate-source capacitance.

Mobilities were derived from dc transistor characteristics in the following manner. At small drain bias  $V_D$ , the conductance between source and drain can be approximated as<sup>7</sup>

$$g_D = \frac{I_D}{V_D} = q\mu n_s \frac{W}{L}, \quad (1)$$

where  $I_D$  is the drain current,  $q$  the electron charge,  $\mu$  the mobility of the electrons in the channel,  $n_s$  the total sheet carrier concentration, and  $W$  and  $L$  the width and length of the gate, respectively. Low-field mobilities can be derived from measurements of  $g_D$  and  $n_s$ . The results for  $V_D = 50\ \text{mV}$  are shown in Fig. 2 as a function of  $V_g$ . The mobility values range from 420 to  $1100\ \text{cm}^2/\text{V}\cdot\text{s}$ , which are comparable with reported values of Hall mobility for an  $\text{Al}_x\text{Ga}_{1-x}\text{N}/\text{GaN}$  heterostructure.<sup>8,9</sup>

For positive gate bias, mobility decreases with increasing gate bias; we attribute this decrease to spillover of electrons into the  $\text{Al}_{0.15}\text{Ga}_{0.85}\text{N}$  layer, which provides a parallel conduction path in addition to the 2DEG. In this case, the total mobility and sheet carrier concentration are given by

$$\begin{aligned} \mu &= (n_{2\text{DEG}}\mu_{2\text{DEG}} + n_{\text{AlGaIn}}\mu_{\text{AlGaIn}})/n_s, \\ n_s &= n_{2\text{DEG}} + n_{\text{AlGaIn}}, \end{aligned} \quad (2)$$

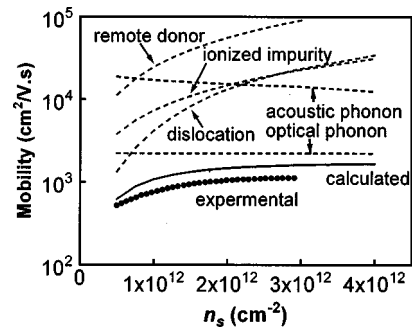


FIG. 3. Experimental (solid circles) and calculated (solid line) mobility as a function of sheet carrier concentration in the 2DEG at 300 K. The calculated mobilities associated with individual scattering are shown by dashed lines.

where  $n_{2\text{DEG}}$  and  $n_{\text{AlGaIn}}$  are the sheet carrier concentrations in the 2DEG and in the  $\text{Al}_{0.15}\text{Ga}_{0.85}\text{N}$  layer, respectively.

Given the values for  $n_{2\text{DEG}}$  and  $n_{\text{AlGaIn}}$  obtained from the simulations described above, the measured mobility for positive gate bias has been fitted using Eq. (2) with  $\mu_{2\text{DEG}}$  and  $\mu_{\text{AlGaIn}}$  as fitting parameters. The open circles in Fig. 2 correspond to calculated mobility values for  $\mu_{2\text{DEG}} = 1100 \pm 20\ \text{cm}^2/\text{V}\cdot\text{s}$  and  $\mu_{\text{AlGaIn}} = 100 \pm 20\ \text{cm}^2/\text{V}\cdot\text{s}$ . The good agreement between the measured and fitted mobilities suggests that parallel conduction in the  $\text{Al}_{0.15}\text{Ga}_{0.85}\text{N}$  layer is the dominant reason for the reduction in mobility with increasing  $V_g$  for positive gate bias. Intersubband and interface roughness scattering<sup>10</sup> may also be expected to contribute to mobility changes in this regime.

In the region of negative gate bias in Fig. 2, the change in mobility is attributed primarily to the change in sheet carrier concentration in the 2DEG. The solid circles in Fig. 3 show mobilities measured at 300 K as a function of sheet carrier concentration in the 2DEG, which is derived by converting the negative gate bias into sheet carrier concentration. The mobility increases substantially with increasing sheet carrier concentration, then eventually saturates for  $n \geq 2 \times 10^{12}\ \text{cm}^{-2}$ . This dependence is similar to that observed for the mobility in the 2DEG at an  $\text{AlGaAs}/\text{GaAs}$  heterojunction at relatively low temperatures.<sup>11</sup> We have calculated the mobility in our device taking into account the carrier scattering by remote donors in the barrier layer, background residual ionized impurities in the GaN layer, acoustic phonons,<sup>12,13</sup> polar optical phonons<sup>14</sup> and threading dislocations.<sup>15</sup> The mobility limits associated with each scattering mechanism are shown in Fig. 3 together with the total mobility determined by Matthiessen's law. The densities of dislocations and ionized impurities are assumed to be  $4 \times 10^8\ \text{cm}^{-2}$  and  $2 \times 10^{17}\ \text{cm}^{-3}$ , respectively. Although there is a difference in the magnitude between the calculated and measured mobilities, the calculated and measured dependences of mobility on carrier concentration are in good agreement. At low sheet carrier concentrations, scattering by dislocations and ionized impurities is important. With increasing sheet carrier concentration, scattering by these mechanisms is reduced due to screening, and polar optical phonon scattering gradually becomes dominant.

The dependence of mobility on temperature has also been investigated. Figure 4 shows the mobility at sheet carrier concentrations of  $8 \times 10^{11}$  and  $2.6 \times 10^{12}\ \text{cm}^{-2}$  as a function of temperature. As shown in Fig. 4, the mobility de-

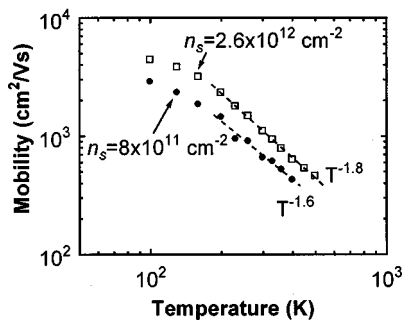


FIG. 4. Mobility at sheet carrier concentrations of  $8 \times 10^{11} \text{ cm}^{-2}$  (solid circles) and  $2.6 \times 10^{12} \text{ cm}^{-2}$  (open squares) as a function of temperature.

creases monotonically with increasing temperature for temperatures ranging from 100 to 500 K. For temperatures of 200–400 K, the mobility varies approximately as  $T^{-\alpha}$ , with  $\alpha=1.8$  for a sheet carrier concentration of  $2.6 \times 10^{12} \text{ cm}^{-2}$ , and  $\alpha=1.6$  for a sheet carrier concentration of  $8 \times 10^{11} \text{ cm}^{-2}$ ; this behavior suggests that phonon scattering is the dominant scattering mechanism at high temperature, in agreement with a number of previous studies.<sup>13,14</sup> The reduced dependence of mobility on temperature for the lower carrier concentration suggests that scattering by dislocations and defects is more significant for lower carrier concentrations, consistent with the calculations shown in Fig. 3.

In summary, we have measured the low-field mobility of electrons in the channel of an  $\text{Al}_{0.15}\text{Ga}_{0.85}\text{N}/\text{GaN}$  HFET by analysis of dc transistor characteristics. The measured mobility is found to decrease with increasing gate bias for positive gate bias voltage; detailed comparison between experimental results and numerical simulations indicates that this is a consequence of parallel conduction in the  $\text{Al}_{0.15}\text{Ga}_{0.85}\text{N}$  layer. For negative gate bias voltage, the mobility is found to increase with increasing gate bias, which we interpret as a

consequence of increased screening of scattering by ionized impurities and dislocations with increasing sheet carrier concentration in the 2DEG. The mobility is found to decrease monotonically with increasing temperature, and varies as  $T^{-\alpha}$  with  $\alpha \approx 1.6\text{--}1.8$  for temperatures ranging from 200 to 400 K.

Part of this work was supported by BMDO (Dr. Kepi Wu) monitored by USASMDC. One of the authors (E.T.Y.) would like to acknowledge financial support from the Alfred P. Sloan Foundation.

- <sup>1</sup>Q. Chen, J. W. Yang, R. Gaska, M. Asif Khan, M. S. Shur, G. J. Sullivan, A. L. Sailor, J. A. Higgins, A. T. Ping, and I. Adesida, *IEEE Electron Device Lett.* **19**, 44 (1998).
- <sup>2</sup>G. J. Sullivan, M. Y. Chen, J. A. Higgins, J. W. Yang, Q. Chen, R. L. Pierson, and B. T. McDermott, *IEEE Electron Device Lett.* **19**, 198 (1998).
- <sup>3</sup>Y. F. Wu, B. P. Keller, P. Fini, S. Keller, T. J. Jenkins, L. T. Kehias, S. P. Denbaars, and U. K. Mishra, *IEEE Electron Device Lett.* **19**, 50 (1998).
- <sup>4</sup>S. C. Binari, J. M. Redwing, G. Kelner, and W. Kruppa, *Electron. Lett.* **33**, 242 (1997).
- <sup>5</sup>E. T. Yu, G. J. Sullivan, P. M. Asbeck, C. D. Wang, D. Qiao, and S. S. Lau, *Appl. Phys. Lett.* **71**, 2794 (1997).
- <sup>6</sup>G. L. Snider, computer program *1D Poisson/Schrödinger: a band diagram calculator*, University of Notre Dame, Notre Dame, IN, 1995.
- <sup>7</sup>S. M. Sze, *Physics of Semiconductor Devices*, 2nd ed. (Wiley, New York, 1981), p. 440.
- <sup>8</sup>M. Asif Khan, Q. Chen, C. J. Sun, M. S. Shur, and B. L. Gelmont, *Appl. Phys. Lett.* **67**, 1429 (1995).
- <sup>9</sup>J. M. Redwing, M. A. Tischler, J. S. Flynn, S. Elhamri, M. Ahoujja, R. S. Newrock, and W. C. Mitchel, *Appl. Phys. Lett.* **69**, 963 (1996).
- <sup>10</sup>R. Oberhuber, G. Zandler, and P. Vogl, *Appl. Phys. Lett.* **73**, 818 (1998).
- <sup>11</sup>K. Hirakawa and H. Sakaki, *Phys. Rev. B* **33**, 8291 (1986).
- <sup>12</sup>P. J. Price, *Surf. Sci.* **143**, 145 (1984).
- <sup>13</sup>L. Hsu and W. Walukiewicz, *Phys. Rev. B* **56**, 1520 (1997).
- <sup>14</sup>M. Shur, B. Gelmont, and M. Asif Khan, *J. Electron. Mater.* **25**, 777 (1996).
- <sup>15</sup>T. Ohori, S. Ohkubo, K. Kasai, and J. Komeno, *J. Appl. Phys.* **75**, 3681 (1994).